Pump-dump control and the related transient absorption spectroscopies

Zhenwen Shen and YiJing Yan[a)]
Department of Chemistry, Hong Kong University of Science and Technology, Hong Kong

Jixin Cheng and Feng Shuang
Department of Chemistry, Hong Kong University of Science and Technology, Hong Kong and Laboratory of Bond-Selective Chemistry, of Science and Technology of China, Hefei, China

Yi Zhao and Guozhong He
Department of Chemistry, Hong Kong University of Science and Technology, Hong Kong and Laboratory of Molecular Reaction Dynamics, Dalian Institute of Chemical Physics, Dalian, China

(Received 27 October 1998; accepted 15 January 1999)

We combine theories of optimal pump-dump control and the related transient probe absorption spectroscopy in order to elucidate the relation between these two optical processes and the possibility of experimental realization. In the weak response regime, we identify the globally optimal pair of pump-dump control fields, and further propose a second-order difference detection scheme to monitor the wave packets dynamics that is jointly controlled by both the pump and dump fields. The globally optimal solution serves also as the initial input for the iterative search for the optimal control fields in the strong response regime. We use a model I_2 molecule to demonstrate numerically the pump-dump control and the detection of a highly vibrationally excited wave packet focusing dynamics on the ground X surface in both the weak and strong response regimes. The I_2B surface serves as the intermediate to assist the pump-dump control and the optical detection processes. Demonstrated in the strong response regime are the optimal pair of pump-dump molecular-π pulses that invert nearly total population onto the predefined target region within a half period of vibration motion. © *1999 American Institute of Physics.* [S0021-9606(99)00115-4]

I. INTRODUCTION

Recent advancement in both theory and experiment has made it possible to use tailored light to attain laser control of chemical dynamics and reactivity in a variety of systems. The basic idea is to exploit the time-frequency coherence of light to actively interfere with the quantum matter wave as it evolves.

The simplest example of active control in time domain is the Tannor-Rice pump-dump control scheme,[1,2] in which reaction selectivity is achieved by the proper timing of the second (dump) light pulse to coincide with the evolution of a pump-excited molecule into desired product Franck–Condon region. Experimental demonstration of this simple time-domain control has been performed by several groups.[3–5] In Tannor and Rice's original work,[1,2] the shape of dump field was also optimized with respect to a fixed pump field in the weak response regime. Paramonov and Manz and their co-workers[6,7] have described a control scheme that uses a sequence of pulses with optimized field strength, frequency, time delay, and duration for each subpulse.

The principle of active control in the frequency domain has been beautifully demonstrated by Brumer and Shapiro.[8–10] They have proposed to use two or more continuous wave (cw) fields to coherently interfere with a degenerate molecular doorway state which may lead to two or more final possible outcomes of a reaction. In the Brumer–Shapiro coherent control scheme, the selectivity of a particular reaction channel is regulated by the relative phase, amplitude, and polarization of two (or more) incident cw fields. This coherent control scheme has been experimentally demonstrated by several groups.[11–15]

A number of methods based on formal control theory, first introduced by Rabitz and co-workers,[16–18] have been presented to determine the coherent temporal-spectral shape of light field that best drives a quantum system to a desired target.[19–28] Experimental demonstrations of the optimal control scheme have been carried out for manipulating the excited state wave packet focusing dynamics and photodissociation product.[29–31] Recently, Yan and co-workers[32–36] have further developed the theory of optimal control via a pair of phase-unlocked coherent fields. This work generalizes the Tannor–Rice pump-dump (or pump-pump) control scheme[1,2] with simultaneous optimization of the pair of phase-unlocked or nondegenerate coherent fields in both the weak and the strong response regimes. Numerical demonstrations have been made on the weak pump-dump control of localized Gaussian wave packets in a high vibrationally excited region on the ground electronic surface.[32–35]

In this paper, we shall consider the possible detection schemes based on the transient absorption spectroscopies to monitor the pump-dump controlled wave packet dynamics in both weak and strong response regimes. For the purpose of demonstration, we consider a generic two-surface molecular system that easily lends itself to a clear discussion of typical pump-dump-probe experiments (cf. Fig. 1).

a)Author to whom correspondence should be addressed; electronic mail: yyan@ust.hk

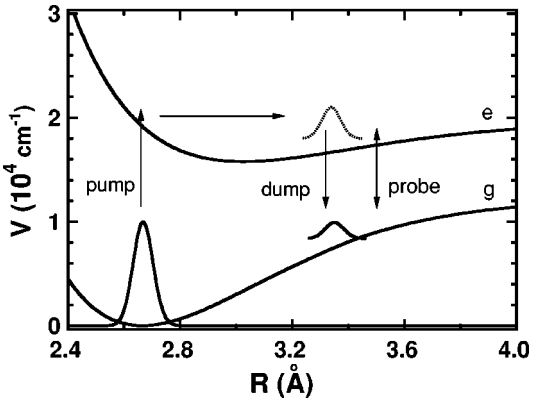

FIG. 1. Schematic diagram of pump-dump-probe control and detection processes.

Let us start with the physical picture of the excitation and detection processes in the weak response regime. In a conventional transient probe absorption measurement, the nonstationary wave packet is induced via a single excitation field, i.e., the pump. Upon excitation, a ''particle'' wave packet is created on the excited surface, while a ''hole'' is left in the initial ground state. In the weak response regime, the excited-surface ''particle'' and the ground-surface ''hole'' may be described by $|\psi_e^{(1)}|^2$ and $\mathrm{Re}[\psi_g^{(0)}\psi_g^{(2)}]$, respectively. Both of them are nonstationary and linearly depend on the intensity of the pump excitation field. We may thus classify $|\psi_e^{(1)}|^2$ as the first-order ''particle'' on the excited surface and $\mathrm{Re}[\psi_g^{(0)}\psi_g^{(2)}]$ the first-order ''hole'' on the ground surface. The evolutions of these nonstationary wave packets on both surfaces are then monitored with a varying delayed probe pulse in terms of transient absorption signals. In a pump-dump-probe optical process, the excitation fields consist of a pair of pump-dump light pulses, rather than a single pulse in the conventional pump-probe experiment. In this case, generated are also a secondary ''particle'' $[|\psi_g^{(2)}|^2]$ on the ground surface and a secondary ''hole'' $\mathrm{Re}[\psi_e^{(1)}\psi_e^{(3)}]$ on the excited surface. These secondary wave packets depend bilinearly on the product of pump and dump intensities. The evolution of the secondary ''particle'' $|\psi_g^{(2)}|^2$ in a highly vibrationally excited region on the ground surface may be monitored via transient laser-induced-fluorescence signals by further pumping it onto the third or another high-lying electronic state surface. However, in an absorption process involving only two surfaces, the transient signals of the secondary ''particle'' $|\psi_g^{(2)}|^2$ are buried in the much stronger signals of the first-order ''particle'' $|\psi_e^{(1)}|^2$. In this work, we propose a simple second-order difference signal detection scheme [cf. Eq. (30)] that allows us to eliminate the first-order signal contributions. We shall also demonstrate how the control theory is applied to design the globally optimal pump-dump field pair that drives the secondary ''particle'' $|\psi_g^{(2)}|^2$ to best overlap with a predefined target wave packet at a given target time.

In the strong response regime, the total inversion of population into the target region may be obtained. The pump-dump control of total population inversion considered here has two exotic characteristics. First, the excitation fields consist of a pair of molecular-π pulses. The molecular-π pump pulse achieves the total population inversion of the initially stationary ground surface molecular sample onto the electronic surface. The subsequent molecular-π dump pulse reverses the processes by inverting the nonstationary excited surface wave packet completely back to the ground surface target region. Second, the pair of molecular-π pulses should be properly shaped and timed such that they jointly and optimally drive the molecular wave packet into the predefined target distribution in the nuclear phase-space at the specified target time. In this work, we shall present a numerical example of a pair of nearly perfect molecular-π pump-dump pulses that achieve over 90% of total population inversion in the above mentioned controlled manner.

The remainder of this paper is organized as follows. In Sec. II, we outline our previous theoretical results on the optimal pump-dump control in a two-surfaces molecular system.[32–35] In Sec. III, we present the theory of transient weak probe absorption in the presence of arbitrary excitation fields. Due to the same dynamics processes involved, a great similarity between the formulation of optimal pump-dump control and that of transient absorption is expected. In Sec. IV, we demonstrate the control and detection of nuclear wave packet focusing dynamics of a model I_2 molecule on both the excited and ground surfaces and in both the weak and the strong response regimes. Finally, we summarize and conclude in Sec. V.

II. THEORY OF OPTIMAL CONTROL

A. General theory in the strong response regime

Consider a laser excitation process in a molecule system involving the ground g and an excited e electronic states (cf. Fig. 1). The total Hamiltonian in the electronic rotating-wave-approximation (RWA) assumes the form

$$H(t)=H_0-D_+E(t)-D_-E^*(t), \tag{1a}$$

$$H_0=H_g|g\rangle\langle g|+H_e|e\rangle\langle e|, \tag{1b}$$

$$D_+=\mu|e\rangle\langle g| \quad \text{and} \quad D_-=\mu|\rangle\langle e|. \tag{1c}$$

Here, H_g and H_e are the adiabatic Hamiltonians for the molecular nuclear dynamics, and μ is the electronic transition dipole moment which depends generally on the molecular configuration. D_+ and $D_-=D_+^\dagger$ can physically be viewed as the creation and annihilation operators, respectively, for the electronic excitation or exciton. They satisfy the following relations: $D_+|g\rangle=\mu|e\rangle$, $D_-|e\rangle=\mu|g\rangle$, and $D_-|\rangle=D_+|e\rangle=0$. In Eq. (1), $E(t)$ denotes the external field envelope, which is considered as a given input in a spectroscopic problem (cf. Sec. III) but an undetermined function in a control process. Note in Eq. (1) all operators can be equally written in the matrix form. For example,

$$H(t)=\begin{bmatrix} H_g & -\mu E^*(t) \\ -\mu E(t) & H_e \end{bmatrix}. \tag{2}$$

Similarly, the two-surface wave function $\psi(t)$ governed by the Hamiltonian $H(t)$ can be written as

$$\psi(t)\equiv G(t,t')\psi(t')=\begin{bmatrix}\psi_g(t)\\ \psi_e(t)\end{bmatrix}. \tag{3}$$

In this paper we consider the control problem in which the target is chosen as a pure state $|\phi\rangle$. We shall search for the optimal field $E(t)$ that best drives the molecular system wave packet $\psi(t)$ to overlap with the target at a specified target time t_f. We shall consider the simplest constraint that the incident intensity,

$$I=\int_0^{t_f} dt|E(t)|^2, \tag{4}$$

from the control remains finite and nonzero. In this case, the control problem is a functional optimization of the following quantity:[16,17,20,21]

$$J[\{E(t)\};t_f]=|c(t_f)|^2-\lambda I, \tag{5}$$

with respect to the control field function $E(t)$. In Eq. (5), λ is the constant Lagrangian multiplier for the constraint of a finite incident field intensity I [Eq. (4)], while $c(t_f)$ is the control yield amplitude defined as

$$c(t)\equiv\langle\phi|\psi(t)\rangle. \tag{6}$$

To find the control equation that determines the optimal $E(t)$, we shall consider the variation in control yield, $\delta|c(t_f)|^2$, with respect to the variation in control field. Using the first-order perturbation theory in the Hilbert space, we obtain

$$\begin{aligned}\delta|c(t_f)|^2&=c(t_f)\,\delta c^*(t_f)+c^*(t_f)\,\delta c(t_f)\\ &=\int_0^{t_f} dt[c(t_f)f_+^*(t;t_f)\\ &\quad+c^*(t_f)f_-(t;t_f)]\delta E^*(t)+\text{c.c.}\end{aligned} \tag{7}$$

Here, c.c. stands for the complex conjugate,

$$f_\pm(t;t_f)=(i/\hbar)\langle\phi|G(t_f,t)|\psi_\pm(t)\rangle, \tag{8}$$

and

$$\psi_\pm(t)\equiv D_\pm\psi(t). \tag{9}$$

In Eq. (8), $G(t_f,\tau)$ is the Hilbert-space propagator governed by the total Hamiltonian $H(t)$ [Eq. (1)] in the presence of the control field. The final control equation can then be obtained by using the variation principle $\delta J=0$ together with Eq. (7). We have[16,20,32–35]

$$c(t_f)f_+^*(t;t_f)+c^*(t_f)f_-(t;t_f)=\lambda E(t). \tag{10}$$

The key quantities here are f_+ and f_- [Eq. (8)] that carry all the t-dependent information required by the optimal field. The evaluation of $f_\pm$ involves the propagation of wave packet under the Hamiltonian $H(t)$ [Eq. (1)] in the presence of control field $E(t)$. Thus, Eq. (10) is nonlinear and should be solved iteratively for the locally optimal field $E(t)$ at any given intensity.

As D_+ and D_- [Eq. (1c)] are the exciton creation and annihilation operators, f_+ and f_- can actually be viewed as the Hilbert-space pump and dump control kernel, respectively. This distinction constitutes the background for the theory of pump-dump control via a pair of phase-unlocked pump-dump $\{E_p,E_d\}$ fields. In this case, the control equations assume[32–35]

$$\langle c(t_f;\theta)f_+^*(t;t_f,\theta)\rangle=\lambda_p E_p(t), \tag{11a}$$

$$\langle c^*(t_f;\theta)f_-(t;t_f,\theta)e^{i\theta}\rangle=\lambda_d E_d(t). \tag{11b}$$

Here, λ_p and λ_d are the constant Lagrangian multipliers for the constraints of finite incident intensities from the pump and the dump control fields, respectively. In Eq. (11), the control amplitude c and the control kernel $f_\pm$ are evaluated with the Hamiltonian $H(t)$ of Eq. (1) in the presence of $E(t)=E_p(t)+e^{-i\theta}E_d(t)$, the coherence superposition of the pump-dump fields that are phase-locked at the specified phase θ. The final coupled control equations for the optimal pair of phase-unlocked fields should include the ensemble average $\langle\cdots\rangle$ over the random phase θ distribution.

B. Linear theory in the weak response regime

As mentioned earlier, the general equation in either the phase-locked [Eq. (10)] or phase-unlocked [Eq. (11)] control scheme is nonlinear and should be solved in an iterative manner. The converged solution is, however, only locally optimal and depends generally on the input field to initialize the time consuming iterative procedure. Moreover, locally optimal fields tend often to be too complicated to be experimentally realizable. To facilitate this problem, there has been much effort directed toward the linear versions of control theory.[25,35–39] In the following we shall describe two limiting cases in the weak control response regime in which the linear versions of control theory can be generally obtained.[32]

Before proceeding, let us analyze the power law of the relevant quantities c and $f_\pm$ in the general Hilbert-space control theory [Eq. (10) or Eq. (11)] in the weak response regime. The other commonly used terminology for the weak response regime is the n-photon processes in which the leading term in the control amplitude c [Eq. (6)] depends on the external field E (or E^*) to the nth order. In this case, the Hilbert-space control kernel f_+ or f_- depends on the field to the $(n-1)$th order [cf. Eq. (7)]. It concludes that the linear control theory can be obtained not only in the one-photon processes, but also in the two-photon weak response regime.

1. Solution to the one-photon excitation control

Let us consider the control of an excited surface target $\phi=\phi_e|e\rangle$ via the one-photon excitation process in the weak response regime. Hereafter, we shall also assume that the molecule is initially in an eigenstate $\psi(0)=\nu|g\rangle$ on the ground surface. In order to simplify the notation, the eigenenergy ϵ_ν of the initial state is chosen to be the energy zero. The relevant quantities in the one-photon control regime can thus be evaluated as

$$f_+^0(t,t_f)=(i/\hbar)\langle\phi_e|e^{-iH_e(t_f-t)/\hbar}\mu|\nu\rangle, \tag{12a}$$

$$f_-^{(0)}(t,t_f)=0, \tag{12b}$$

$$c^{(1)}(t_f)=\int_0^{t_f} dt f_+^{(0)}(t,t_f)E(t). \tag{12c}$$

Substituting the above equations to Eq. (10) followed by neglecting the trivial constant and phase, we obtain the following solution to the optimal one-photon control field in the weak response regime[1,32]:

$$E(t)=\langle \phi_e|e^{-iH_e(t_f-t)/\hbar}\mu|\nu\rangle^*. \tag{13}$$

This is the time-dependent Franck–Condon overlap between the initial state $|\nu\rangle$ and the free-backward-propagated target state $\langle \phi_e^{(0)}(t;t_f)|\equiv\langle \phi_e|e^{-iH_e(t_f-t)/\hbar}$ on the excited surface.

2. Eigenequation for the two-photon pump-dump control

We shall now consider the control of a ground surface target $\phi=\phi_g|g\rangle$ via the two-photon pump-dump excitation in the weak response regime. In this case, the relevant quantities are[32,33,39]

$$f_+^{(1)}(t,t_f)=(i/\hbar)\langle \phi_e^{(1)}(t,t_f)|\mu|\psi_g^{(0)}(t)\rangle = \int_t^{t_f} dt' B(t',t)E^*(t'), \tag{14a}$$

$$f_-^{(1)}(t,t_f)=(i/\hbar)\langle \phi_g^{(0)}(t,t_f)|\mu|\psi_e^{(1)}(t)\rangle = \int_0^{t} dt' B(t,t')E(t'), \tag{14b}$$

$$c^{(2)}(t_f)=\int_0^{t_f}dt\int_0^t dt' E^*(t)B(t,t')E(t') = \int_0^{t_f} dt f_-^{(1)}(t,t_f)E^*(t) = \int_0^{t_f} dt f_+^{(1)}(t,t_f)E(t). \tag{14c}$$

Here, $B(t,t')$ is the Hilbert-space pump-dump control response function defined by[32,33,39]

$$B(t,t')=\begin{cases}\langle \phi_g^{(0)}(t;t_f)|\hat{T}(t-t')|\nu\rangle; & \text{for } t\geqslant t' \\ 0 \quad \text{for } t<t'\end{cases}. \tag{15}$$

In this equation, $\langle \phi_g^{(0)}(t;t_f)|\equiv\langle \phi_g|e^{-iH_g(t_f-t)/\hbar}$ is the free-backward-propagated ground state target. The two-photon $\hat{T}$ operator is defined as

$$\hat{T}(t)\equiv(i/\hbar)^2\mu e^{-iH_e t/\hbar}\mu. \tag{16}$$

We notice that there is a simple scaling relation between $c^{(2)}(t_f)$ and $f_\pm^{(1)}(t;t_f)$ [Eq. (14c)]. Owning to this relation, the phase of $c^{(2)}(t_f)$ becomes irrelevant to the control process and can be completely removed from the control equation. In this case, the linearized version of Eq. (10) can be cast as[32,33,39]

$$\int_0^{t_f} dt'[B^*(t',t)+B(t,t')]E(t')=\lambda E(t). \tag{17}$$

In the time-grid representation, the optimal field $E(t)$ is a vector of N elements, while $B(t,t')$ is a lower-trigonal $N\times N$ matrix. Equation (17) can thus be recast in the standard form of the Hermitian matrix eigenequation: $(\mathbf{B}^\dagger+\mathbf{B})E=\lambda E$.

By using Eq. (17), we can further cast the control amplitude $c^{(2)}$ [Eq. (14c)] in the weak response regime as[32,33]

$$c^{(2)}(t_f)=\int_0^{t_f}dt\int_0^{t_f}dt' E^*(t)B(t,t')E(t')=\frac{\lambda I}{2}. \tag{18}$$

This equation states that the eigenvalue of Eq. (17) is the control yield amplitude with respect to the incident field intensity: $\lambda\propto|c^{(2)}(t_f)|/I$. The globally optimal field in the two-photon weak control response regime can thus be obtained as the eigenfunction of Eq. (17) associating with the largest eigenvalue. Note that by using the optimal field [Eq. (17)], the two-photon control amplitude $c^{(2)}(t_f)$ is real and positive at the target time t_f. This is consistent with the choice of setting $\arg[c^{(2)}(t_f)]=0$ in the derivation of Eq. (17).

To conclude this section, let us further present the control equations for the optimal pair of phase-unlocked pump-dump fields $\{E_p,E_d\}$ in the weak response regime [cf. Eq. (11)]. They are given by[32,33,35]

$$\int_0^{t_f} dt'[B^\dagger B](t,t')E_p(t')=\lambda_{pd}E_p(t), \tag{19a}$$

$$\int_0^{t_f} dt'[BB^\dagger](t,t')E_d(t')=\lambda_{pd}E_d(t). \tag{19b}$$

Here,

$$[B^\dagger B](t,t')\equiv\int_0^{t_f}dt'' B^*(t'',t)B(t'',t'), \tag{20}$$

and $[BB^\dagger](t,t')$ is defined similarly. The common eigenvalue λ_{pd} in Eq. (19) associates with the control yield with respect to product of the incident intensities from both the pump and the dump fields

$$\lambda_{pd}=|c^{(2)}(t_f)|^2/(I_pI_d). \tag{21}$$

Therefore, the globally optimal phase-unlocked pump-dump field pair $\{E_p,E_d\}$ can be identified as the eigenfunctions of Eq. (19) associating with the largest eigenvalue.

III. THEORY OF TRANSIENT ABSORPTION

We shall now consider the formulation of weak transient probe absorption spectroscopies in the presence of arbitrary external excitation fields, such as the optimal pump-dump fields presented in the previous section. In general, the probe absorption signal $S(t_T)$ can be expressed in terms of $P(\mathbf{k}_T,t)$, the optical polarization at the probe field direction. We have[40–42]

$$S(t_T)=2\ \mathrm{Im}\int_{-\infty}^{\infty}dtE_T^*(t-t_T)P(\mathbf{k}_T,t) \equiv 2\ \mathrm{Im}\int_{-\infty}^{\infty}dtE_T^*(t-t_T) \times\int d\mathbf{r}e^{-i(\mathbf{k}_T\mathbf{r}-\Omega_T t)}\langle\psi_T(t)|D_-|\psi_T(t)\rangle. \tag{22}$$

In this equation, $E_T(t-t_T)$ and Ω_T are, respectively, the complex envelope and the carrier frequency of the probe field that centers at $t=t_T$. In the calculation of conventional

pump-probe spectroscopy, the pump field is taken to be centered at $t=0$, and therefore t_T denotes the probe delay time. In this work, t_T is referred to the probing time with respect to the beginning of control.

In the weak probe response regime, we can approximate the total wave function ψ_T by its first-order perturbation in the matter-probe field interaction. After some simple algebra, we obtain the following formulation for calculating the transient weak probe absorption in the presence of arbitrary excitation fields:

$$S(t_T)=2\ \mathrm{Im}\int_{-\infty}^{\infty}dt\int_0^{\infty}d\tau e^{i\Omega_T\tau}E_T(t)E_T^*(t+\tau)\times[R_+(\tau,t_T+t)+R_-^*(\tau,t_T+t)]\equiv S_g(t_T)+S_e(t_T), \tag{23}$$

with

$$R_{\pm}(\tau,t)=(i/\hbar)\langle\psi_{\pm}(t+\tau)|G(t+\tau,t)|\psi_{\pm}(t)\rangle. \tag{24}$$

In the second identity of Eq. (23), we denote explicitly the total transient signals as the sum of two contributions. One is S_g evaluated from Eq. (23) with only the R_+ term, and another is S_e with only R_-. Note that $\psi_{\pm}$ [Eq. (9)] can be recast in the matrix form as

$$\psi_+(t)\equiv D_+\psi(t)=\begin{bmatrix}0\\ \mu\psi_g(t)\end{bmatrix}, \tag{25a}$$

$$\psi_-(t)\equiv D_-\psi(t)=\begin{bmatrix}\mu\psi_e(t)\\ 0\end{bmatrix}. \tag{25b}$$

In this sense, $R_+(\tau,t)$ [cf. Eq. (24)] can be considered as the probe response of the nonstationary wave function $\psi_g(t)$ on the ground surface, while $R_-(\tau,t)$ is that of $\psi_e(t)$ on the excited surface, in the presence of arbitrary excitation fields. In other words, R_+ contributes to the $e\leftarrow g$ absorption [i.e., S_g in the second identity of Eq. (23)], while R_- contributes to the stimulated $e\rightarrow g$ emission signals [i.e., S_e in the second identity of Eq. (23)]. The above physical distinction made to R_+ and R_- is very similar to what we made in Sec. II A to the pump control kernel f_+ and the dump control kernel f_-. Formally, there is also much similarity between the spectroscopic response function $R_{\pm}$ of Eq. (24) and the control response function $f_{\pm}$ of Eq. (8). This underlying similarity in both the physical processes and the formal structure suggests the possibility of using transient probe absorption signals to monitor the pump-dump controlled molecular wave packet dynamics.

IV. NUMERICAL RESULTS

We shall present numerical examples of control and detection of a model I_2 vibrational wave packet dynamics on both the ground X and the excited B surfaces (cf. Fig. 1 with $g=X$ and $e=B$). Their potential functions are taken to be Morse with the parameters listed in Table I. For simplicity, we neglect the effects of molecular rotation and of the non-Condon transition dipole. We set $\mu=1$ Debye. The molecule begins at the vibronic $\nu=0$ level in the ground electronic X state. The target is chosen as a minimum-uncertainty Gaussian wave packet on either the ground or the excited surface.

TABLE I. Parameters for I_2 Morse potential surfaces in the gas phase, $V(R)=T_e+D_e[1-e^{-\beta(R-R_e)}]^2$.

Surface	T_e (cm^{-1})	D_e (cm^{-1})	β ($\mathrm{\AA}^{-1}$)	R_e (Å)
X or g	0	12 550	1.871	2.666
B or e	15 769	4381	1.876	3.016

$$\phi_{g,e}(R)=\exp\left[-\frac{(R-\bar{r})^2}{4\Delta_r^2}-i\frac{\bar{p}}{\hbar}(R-\bar{r})\right]. \tag{26}$$

This target centers at $\bar{r}$ in coordinate with a width of Δ_r, and at $\bar{p}$ in momentum with a width of $\Delta_p=\hbar/2\Delta_r$. The target time is chosen to be $t_f=200$ fs.

In order to illustrate the time-frequency coherence in the optimal control field to be evaluated later, we shall also introduce the Wigner field profile defined as

$$F_W(\omega,t)=2\ \mathrm{Re}\int_0^{\infty}d\tau e^{-i\omega\tau}E^*\left(t+\frac{\tau}{2}\right)E\left(t-\frac{\tau}{2}\right). \tag{27}$$

In the following spectroscopic [Eq. (23)] calculations, all probes are chosen to be transform-limited pulses with the full width at half maximum (FWHM) of 35 fs in $|E_T(t)|^2$. The probe carrying frequency Ω_T in each calculation will be specified.

A. Pump-probe of molecular dynamics

Before presenting the main results of pump-dump-probe processes in the next subsection, let us first discuss some related topics on the simple pump-probe control and detection in the weak response regime. We start with a minimum uncertainty Gaussian target on the excited surface, ϕ_e of Eq. (26). The target parameters are the coordinate center $\bar{r}=3.55$ Å, the coordinate spread $\Delta_r=0.07$ Å, and the momentum mean $\bar{p}>0$ that corresponds to an outgoing kinetic energy of $\bar{p}^2/2m=0.12$ eV. The vibrational period of this target (about 400 fs) is larger than the target time ($t_f=200$ fs). This target is a type of ''molecular paddleball,'' or an outgoing wave packet in the bound potential surface region.[26,34] We shall see in Sec. IV B that the pump-dump control of wave packet focusing dynamics involves the pump prefocusing of a molecular paddleball on the excited state surface.

Figure 2 presents the Wigner profile F_W [Eq. (27)] of the optimal pump excitation field evaluated via Eq. (13) in the weak one-photon control response regime. The figure shows clearly that the optimal pump field for focusing the outgoing wave packet is up-chirped, the average frequency increasing with time. This is consistent with the following classical picture of the process. The lower energy components of matter wave packet are excited by the lower frequency components of light wave packet. These wave packet components carry lower momenta and will take relatively longer times to reach the outgoing target region. Thus, the low-energy wave packet components should be excited before the high-energy components so that the maximum overlap with the highly localized target can be achieved at the given target time.

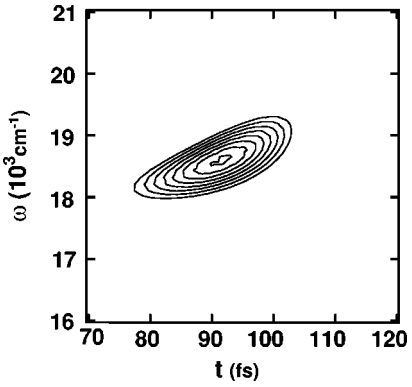

FIG. 2. Wigner time-frequency profile of the optimal (pump) excitation field in the one-photon weak response regime. The control target is an outgoing minimum uncertainty Gaussian wave packet on the excited surface. The target time is $t_f = 200$ fs.

We shall now consider the detection signal measurement in the weak response regime. To examine the effect of pump excitation, the transient signal is usually recorded in the difference scheme,

$$\Delta S(t_T) = S(t_T) - S_0(t_T). \tag{28}$$

Here $S(t_T)$ [Eq. (23)] denotes the signal measured with the excitation field on, while $S_0(t_T)$ is with the field off. In the conventional weak pump-probe spectroscopic processes, the excitation field refers to the pump that creates a nonstationary ''particle'' wave packet $|\psi_e^{(1)}|^2$ on the excited surface, while leaving a nonstationary ''hole'' $\mathrm{Re}[\psi_g^{(0)}\psi_g^{(2)}]$ on the ground surface. Both of them are of the first order, as their intensities depend linearly on the intensity of excitation field. The difference signal $\Delta S(t_T)$ contains in principle both contributions from the particle and the hole. These two contributions correspond to ΔS_e (arising from R_-) and ΔS_g (arising from R_+) in the second identity of Eq. (23), respectively. However, the relative strength of these contributions depends on the probe frequency that defines the window of detection. Demonstrated in Fig. 3 are the transient signals probed at three representative frequencies. In Fig. 3(a), the probe frequency (8090 cm^{-1}) is tuned to the resonance with the target Franck-Condon transient region, at which the ground state ''hole'' is largely off-resonant. In this case, the ΔS_g contribution from the ground state ''hole'' is suppressed and the experimental transient absorption signal, $\Delta S(t_T) = \Delta S_e(t_T)$, monitors the coherent motion of the excited state wave packet. As the target is an outgoing wave packet with the mean momentum $\overline{p} > 0$, the detection window is in between two turning points. Thus, a localized wave packet passes the detection window twice in each period of oscillation, resulting in the appearance of two trains of quantum beats in Fig. 3(a). One is for the bond stretching and another for the bond compression. In Fig. 3(b), the probe frequency (7500 cm^{-1}) is tuned to detect the wave packet dynamics at the outer turning point on the excited surface. In this case, two trains of quantum beats collapse into one. The wave packet at the turning point [cf. the first peak of Fig. 3(b)] is much broader than that in the controlled target region at the control time [cf. the first peak of Fig. 3(a)]. The dispersion of wave packet

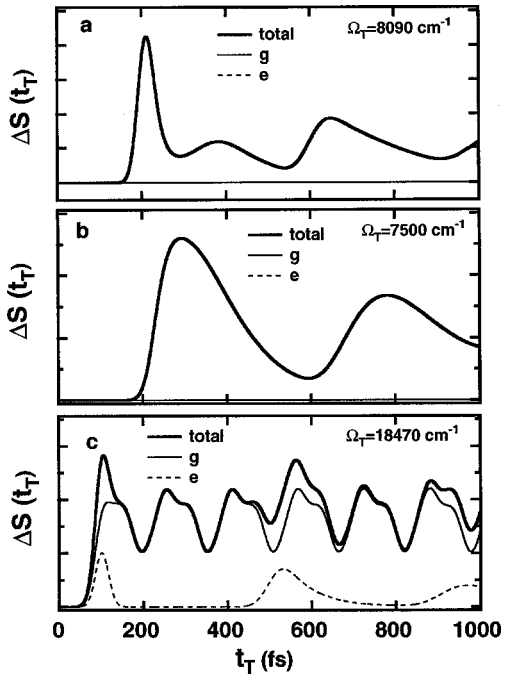

FIG. 3. Conventional difference transient absorption signals [Eq. (28)] at three representative detection frequencies in the presence of the excitation field of Fig. 2. The observed signal (dark-solid) in each panel is a sum of two contributions [Eq. (23)]. One is from the wave packet motion on the ground surface (thin-solid), and another is from that on the excited surface (dashed).

is a natural tendency of molecular anharmonicity. The optimal field with an appropriate chirp is capable of compensating this natural tendency. In Fig. 3(c), the probe frequency (18 470 cm^{-1}) is the same as that of the pump field. In this case, the probe window is near the inner turning point of the excited surface, and is also in resonance with the Franck-Condon transition of ''hole'' wave packet on the ground surface. The contributions from both the ground state ''hole'' (ΔS_g) and the excited ''particle'' (ΔS_e) are substantial. As the ''particle'' is high vibrationally excited with a relative large mean oscillation period, the quantum beat of ground state ''hole'' can still be seen clearly. The appearance of double humps in Fig. 3(c) indicates that the ground state hole may be primarily double peaked in nature.

B. Pump-dump-probe of molecular dynamics

We now turn to the main objective of this paper, the pump-dump control and its related transient absorption spectroscopies. The control target is a high vibrationally excited minimum uncertainty Gaussian wave packet ϕ_g of Eq. (26), on the ground state surface. The parameters for the Gaussian wave packet target are $\overline{r} = 3.35$ Å, $\overline{p} = 0$, and $\Delta_r = 0.03$ Å (Fig. 1). This target is a coherent superposition of about 25 levels, with the center around $\nu = 40$. The mean vibrational energy of this target is about 7450 cm^{-1}. The target time is chosen as $t_f = 200$ fs.

We start with the calculation of the globally optimal pump-dump field (pair) in the weak two-photon response regime. This is done by evaluating the eigenfunction of Eq. (17) or Eq. (19) that corresponds to the largest eigenvalue.

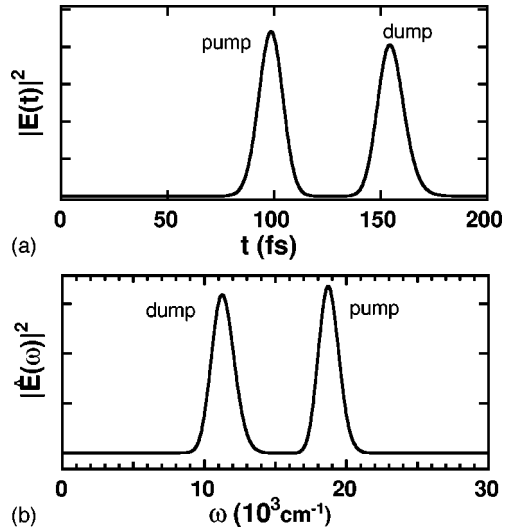

FIG. 4. Temporal (a) and spectral (b) intensity profiles of the globally optimal pump-dump fields pair in the weak response regime.

The resulting pump-dump fields are then used to initiate the iterative solution to Eqs. (10) or (11) for control fields at a certain finite intensity. The converged solution at any given intensity is used as the initial input for the next step of iteration procedure for the optimal pump-dump control fields with a slightly higher intensity. It is found that there is no difference between the phase-locked [Eqs. (10) and (17)] and the phase-unlocked [Eqs. (11) and (19)] pump-dump control schemes, for the target in the field intensity range of consideration in this work. The condition at which phase locking plays a role in control has been analyzed in detail in Ref. 33.

In the following, we shall present the results of optimal pump-dump control at two representing intensities and their corresponding transient probe absorption signals. In the calculations of transient spectroscopies [Eq. (23)], the probe fields are chosen as transform-limited Gaussian pulses with the temporal FWHM$=35$ fs. The probe frequency is $\Omega_T = 9110\,\mathrm{cm}^{-1}$, tuned at resonance with the Franck–Condon transition of the ground state target. Note the mean momentum of the target is zero, $\bar{p}=0$. The probe window is therefore at the outer turning region of the target on the ground potential surface.

1. Pump-dump-probe in the weak response regime

Let us start with the results of the low intensity of the pump-dump control field pair at which each field carries a Rabi flopping angle of 0.3 π. The Rabi flopping angle of a field E_j is defined as $\theta=\int dt\mu|E_j(t)|/\hbar$.[43] We find that at this intensity the optimal fields preserve essentially the globally optimal shapes, i.e., the eigenfunction of Eqs. (17) or (19) corresponding to the largest eigenvalue, in the weak response regime. Figure 4 presents the optimal pair of pump-dump fields in terms of their temporal and spectral intensities. Both fields have simple near-Gaussian form shapes. The Wigner profiles [Eq. (27)] of the optimal pump-dump fields are shown in Fig. 5. Besides an appropriate dump delay with respect to the pump field, the optimal frequency chirp in the pump is positive while that in the dump is negative. This can

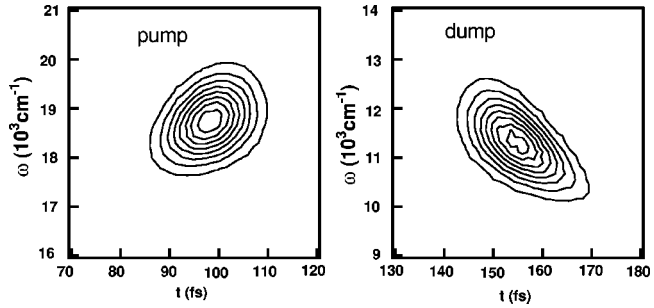

FIG. 5. Wigner intensity profiles of the globally optimal pump-dump control fields pair as in Fig. 4 in the weak response regime.

be understood as follows. Since the target is a focused Gaussian wave packet at the outer turning point on the ground state surface, it is more efficient for the pump process to create a prefocused and outgoing wave packet on the excited surface. As discussed in Fig. 2, the pump control field in this case is positively chirped. Furthermore, as the pumped wave packet moves outward toward the larger internuclear distance at the target region, the potential difference between the two involving surfaces decreases. As a result, a negative chirp is favored to the dump field.

Figure 6 demonstrates the evolutions of pump-dump controlled wave packets on two surfaces in the weak response regime. The ground state wave function consists of two components: $\psi_g=\psi_g'+\psi_g''$. One is the pump-dumped component ψ' arising after the dump field interaction, and another is the unexcited component ψ_g'' remaining in the initial wave packet region. The population distribution is $\{P_g',P_e,P_g''\}=\{0.1,0.2,0.7\}$ at the target time $t_f=200$ fs. Here, P_g' denotes the population being transferred into the ground surface target region, P_e being pumped and left on the excited surface, while $P_g''=1-P_g'-P_e$ is the unexcited part. At the target time, the pump-dumped wave packet ψ_g'

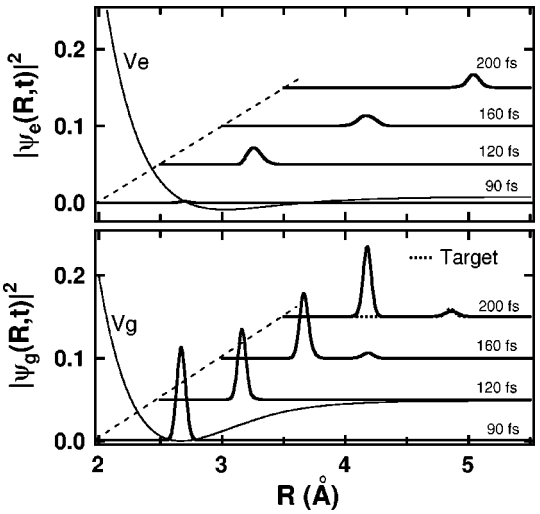

FIG. 6. Evolutions of the wave packets on two surfaces controlled by the globally optimal pump-dump fields pair of Fig. 5. The Rabi flopping angle in each field is 0.3π. About 10% of total population is inverted, reaching an almost perfect overlap with the predefined target (dashed curve) at $t_f = 200$ fs.

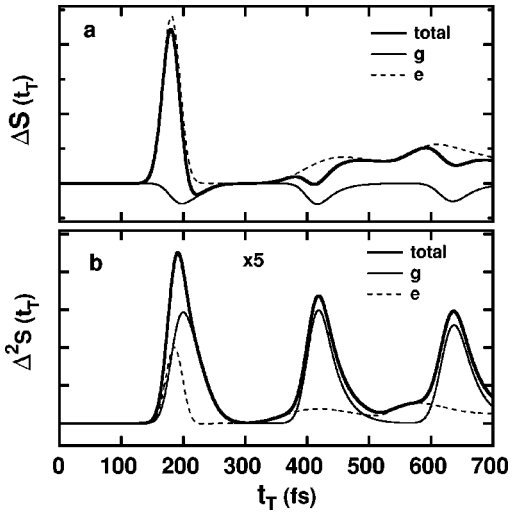

FIG. 7. Transient absorption signals in both the first-order difference scheme ΔS [(a) with Eq. (29)] and the second-order difference scheme $\Delta^2 S$ [(b) with Eq. (30)] for monitoring the controlled wave packet evolutions as shown in Fig. 6. The thin-solid curves are signal contributions from $\psi_g(t)$, while the dashed ones are those from $\psi_e(t)$. The experimental observables (dark-solid) consist of the above two contributions.

overlaps nearly perfectly with the predefined minimum-uncertainty Gaussian target ϕ_g (dashed curve).

Figure 7 depicts the transient absorption signals of the controlled wave packets as shown in Fig. 6. Two difference detection schemes are considered. The upper panel [Fig. 7(a)] shows the conventional first-order difference signals, defined as [cf. Eq. (28)]

$$\Delta S(t_T) = \Delta S_{pd}(t_T) = S_{pd}(t_T) - S_0(t_T). \tag{29}$$

Here, $S_{pd}(t_T)$ is evaluated via Eq. (23) in the presence of both pump and dump fields, while S_0 is that in the absence of both excitation fields. The lower panel [Fig. 7(b)] presents the second-order difference signals defined as

$$\Delta^2 S(t_T) = \Delta S_{pd}(t_T) - \Delta S_p(t_T) - \Delta S_d(t_T). \tag{30}$$

Here, ΔS_p or ΔS_d is the first-order difference signal with only the pump or the dump field, respectively. In the weak response regime, the pump-dumped wave packet on the ground state surface constitutes a second-order ''particle,'' $|\psi_g'|^2 = |\psi_g^{(2)}|^2$, in the highly vibrationally excited region. In the first-order difference detection scheme [Fig. 7(a)], the spectroscopic signature of the second-order ''particle'' dynamics (the thin solid curve) is largely buried in the opposite signal (the dashed curve) arising from the first-order or the pump-excited ''particle'' $|\psi_e^{(1)}|^2$ on the excited surface. In the second-order difference scheme [Fig. 7(b)], the signal contributes from the second-order ''particle'' (the thin solid curve) on the ground surface and the second-order ''hole'' $\mathrm{Re}[\psi_e^{(1)}\psi_e^{(3)}]$ (the dashed curve) on the excited state surface. All the first-order contributions are removed. As the second-order ''particle'' on the ground surface is being optimally controlled and detected, the observed signal [the dark solid curve in Fig. 7(b)] reveals mainly the optical signature of the dynamics of the highly vibrationally excited wave packet on the ground surface. This situation is much like that in Fig. 3(c) where the dynamics on the ground surface is monitored in the presence of an excited surface wave packet.

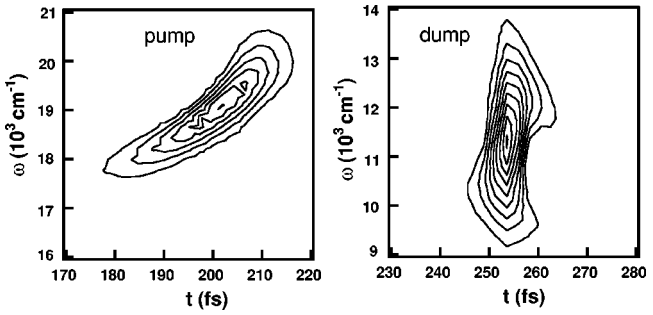

FIG. 8. Wigner intensity profiles of the optimal pump-dump control fields pair in the strong response regime. The Rabi flopping angles of the pump and the dump fields are 1.5 and 0.9π, respectively.

2. Pump-dump-probe in the strong response regime

We shall now consider the strong pump-dump control response regime at which the Rabi flopping angle for the pump field is 1.5 π and that for the dump field is 0.9 π. Figure 8 shows the resulting optimal pair of pump-dump fields evaluated in the iterative manner described in the beginning of Sec. IV B. The optimal fields remain relatively simple shapes as their intensity intensities increase. However, they (Fig. 8) deviate appreciably from the globally optimal shapes (Fig. 5) in the weak response regime. The frequency chirp in the optimal pump field in the strong response regime remains positive but that in the dump approaches zero. In fact the dump field in Fig. 8 approaches the impulsive limit so that the frequency chirp plays no role on the controlled dynamics.

Figure 9 depicts the evolutions of wave packets, $\psi_g(t)$ and $\psi_e(t)$, controlled by the optimal pair of pump-dump control fields as indicated in Fig. 8. At the target time, the pump-dumped wave packet overlaps nearly perfectly with the predefined minimum-uncertainty Gaussian target ϕ_g

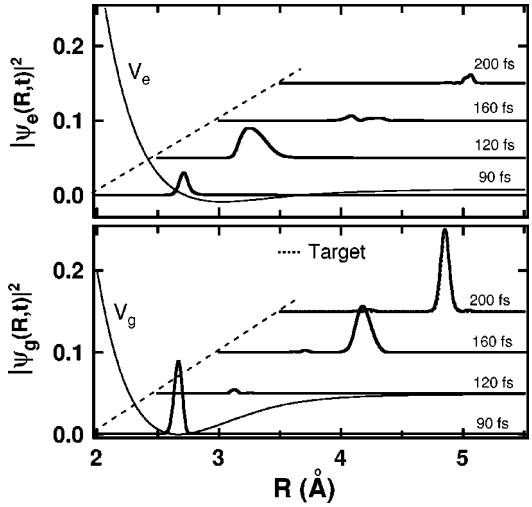

FIG. 9. Evolutions of the wave packets on two surfaces controlled by the optimal pump-dump fields pair of Fig. 8. Over 90% of total population is inverted onto the target region. The controlled wave packet overlaps almost perfectly with the target (dashed curve) at the target time of $t_f = 200$ fs.

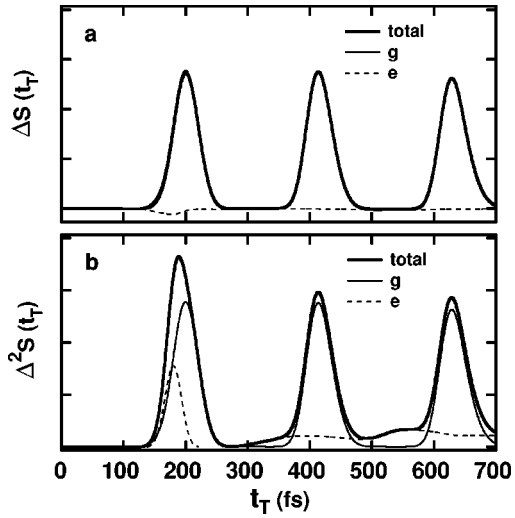

FIG. 10. Same as Fig. 7 but with the pump-dump control fields pair of Fig. 8 in the strong response regime. Wave packet evolutions of Fig. 9 are monitored.

(dashed curve in the lower panel of Fig. 9). The population transfer is $\{P_g', P_e, P_g''\} = \{0.91, 0.075, 0.015\}$, where P_g' denotes the inverted population in the target region, P_e the population being excited onto the excited state surface, and P_g'' the population remains in the initial ground state region. Recall that in a two-level atomic or spin system, a resonant π-pulse inverts 100% of population from the lower level to the upper level.[43] We may refer to the optimal pump-dump fields in Fig. 8 as near the molecular π-pulse pair that invert over 90% of the total population onto the target region (cf. Fig. 9). The molecular pump π-pulse for the total inversion of electronic state population in a molecular system has been recently investigated by Cao *et al.*[44] The studies of molecular pump-dump π-pulse pair for the total inversion of population onto a specified highly vibrationally excited region will be published elsewhere.

Figure 10 shows the corresponding transient signals in both the first-order $\Delta S(t_T)$ [Fig. 10(a) with Eq. (29)] and the second-order $\Delta^2 S(t_T)$ [Fig. 10(b) with Eq. (30)] difference detection schemes. Included in each panel of Fig. 10 are also two signal contributions to the total signal [cf. the second identity of Eq. (23)]. One is from the ground (thin solid curves, arising from R_+) and another is from the excited (dashed curves, arising from R_-) electronic states wave packets. Obviously, the simple first-order difference signal $\Delta S(t_T)$ [Fig. 10(a)] is capable of monitoring the pump-dumped wave packet dynamics in the molecular π-field regime, since almost all population is inverted into the target region. In the weak control response regime we shall, however, consider the second-order difference signal [cf. Fig. 7(b)]. Note the signal strength in the optimal π pump-dump field pair (Fig. 10) is about 200 times larger than that of Fig. 7(b) in the weak response regime.

V. SUMMARY AND CONCLUSION

We have used realistic molecular potentials to demonstrate the optimal pump-dump control in both the strong and weak response regimes and their corresponding transient spectroscopies. The pump-dump field in the weak response regime is calculated via the linear theory of control [Eq. (17) or Eq. (19)] in which the globally optimal solution can be obtained. We have found that the globally optimal pump and dump fields in the weak response regime can efficiently convert over 10% of the total population onto the localized target region at the specified target time. These optimal fields are rather simple and robust for the possibility of experimental realization. We have also proposed a second-order difference detection scheme [Eq. (30) and Fig. 7(b)] to monitor the pump-dump controlled wave packet dynamics in the weak response regime.

The calculations of optimal control fields in the strong response regime are based on the iterative solutions of nonlinear control equations [Eqs. (10) or (11)]. The globally optimal solution in the weak response regime comes naturally as the initial input to start the iterative solutions in the strong response regime. The use of chirped pulses in the strong response regime has proved useful both theoretically[44–46] and experimentally[47,48] in the control of population inversion in multilevel molecular and atomic systems or in the dissipative medium. The effect of chirp is related to the adiabatic passage of the material population dynamics via intensive fields in order to achieve an effective π pulse. Recently, chirped pulses have also been used to study the molecular dynamics and system-bath coupling in solution.[49–51] In this work, we have presented the preliminary results to demonstrate the correlation between the chirps of two optimal fields and the molecular π-field pair for the population inversion onto a localized target region via pump-dump processes.

ACKNOWLEDGMENTS

Support from the Research Grants Council of the Hong Kong Government and the National Natural Science Foundation of China is gratefully acknowledged.

[1] D. J. Tannor and S. A. Rice, J. Chem. Phys. **83**, 5013 (1985).
[2] D. J. Tannor and S. A. Rice, Adv. Chem. Phys. **70**, 441 (1988).
[3] T. Baumert, B. Buhler, M. Grosser, R. Thalweiser, V. Weiss, E. Wiedenmann, and G. Gerber, J. Phys. Chem. **95**, 8103 (1991).
[4] G. G. T. Baumert, Isr. J. Chem. **34**, 103 (1994).
[5] E. D. Potter, J. L. Herek, S. Pedersen, Q. Liu, and A. H. Zewail, Nature (London) **355**, 66 (1992).
[6] G. K. Paramonov and V. A. Savva, Phys. Lett. **97A**, 340 (1983).
[7] W. Jakubetz, B. Just, J. Manz, and H. J. Schreier, J. Phys. Chem. **94**, 2294 (1990).
[8] P. Brumer and M. Shapiro, Faraday Discuss. Chem. Soc. **82**, 177 (1986).
[9] M. Shapiro and P. Brumer, J. Chem. Phys. **84**, 4103 (1986).
[10] M. Shapiro and P. Brumer, Int. Rev. Phys. Chem. **13**, 187 (1994).
[11] R. G. Gordon and S. A. Rice, Annu. Rev. Phys. Chem. **48**, 601 (1997).
[12] L. C. Zhu, V. Kleiman, X. N. Li, S. P. Lu, K. Trentelman, and R. J. Gordon, Science **270**, 77 (1995).
[13] C. Chen and D. S. Elliott, Phys. Rev. Lett. **65**, 1737 (1990).
[14] G. Q. Xing, X. B. Wang, X. Huang, and R. Bersohn, J. Chem. Phys. **104**, 826 (1996).
[15] A. Shnitman, I. Sofer, I. Golub, A. Yogev, M. Shapiro, Z. Chen, and P. Brumer, Phys. Rev. Lett. **76**, 2886 (1996).
[16] A. P. Peirce, M. A. Dahleh, and H. Rabitz, Phys. Rev. A **37**, 4950 (1988).
[17] S. Shi and H. Rabitz, Chem. Phys. **139**, 185 (1989).
[18] H. Rabitz and S. Shi, Adv. Mol. Vibr. Collision Dyn. **1A**, 187 (1991).
[19] W. S. Warren, H. Rabitz, and M. Dahleh, Science **259**, 1581 (1993).
[20] R. Kosloff, S. A. Rice, P. Gaspard, S. Tersigni, and D. J. Tannor, Chem. Phys. **139**, 201 (1989).

[21] S. H. Tersigni, P. Gaspard, and S. A. Rice, J. Chem. Phys. **93**, 1670 (1990).
[22] J. Somlói, V. A. Kazakov, and D. J. Tannor, Chem. Phys. **172**, 85 (1993).
[23] B. Amstrup, J. D. Doll, R. A. Sauerbrey, G. Szabó, and A. Lörincz, Phys. Rev. A **48**, 3830 (1993).
[24] M. Sugawara and Y. Fujimura, J. Chem. Phys. **100**, 5646 (1994).
[25] Y. J. Yan, R. E. Gillilan, R. M. Whitnell, K. R. Wilson, and S. Mukamel, J. Phys. Chem. **97**, 2320 (1993).
[26] J. L. Krause, R. M. Whitnell, K. R. Wilson, Y. J. Yan, and S. Mukamel, J. Chem. Phys. **99**, 6562 (1993).
[27] J. L. Krause, R. M. Whitnell, K. R. Wilson, and Y. J. Yan, in *Femtosecond Chemistry*, edited by J. Manz and L. Wöste (VCH, Weinheim, 1995), pg. 743.
[28] B. Kohler, J. Krause, F. Raksi, K. R. Wilson, R. M. Whitnell, V. V. Yakovlev, and Y. J. Yan, Acc. Chem. Res. **28**, 133 (1995).
[29] B. Kohler, V. V. Yakovlev, J. Che, J. L. Krause, M. Messina, K. R. Wilson, N. Schwentner, R. M. Whitnell, and Y. J. Yan, Phys. Rev. Lett. **74**, 3360 (1995).
[30] C. J. Bardeen, J. Che, K. R. Wilson, V. V. Yakovlev, V. A. Apkarian, C. C. Martens, R. Zadoyan, B. Kohler, and M. Messina, J. Chem. Phys. **106**, 8486 (1997).
[31] C. J. Bardeen, J. Che, K. R. Wilson, V. V. Yakovlev, P. Cong, B. Kohler, J. L. Krause, and M. Messina, J. Phys. Chem. A **101**, 3815 (1997).
[32] Y. J. Yan, Annu. Rep. Prog. Chem., Sect. C: Phys. Chem. **94**, 397 (1998).
[33] Y. J. Yan, Z. W. Shen, and Y. Zhao, Chem. Phys. **233**, 191 (1998).
[34] Y. J. Yan, J. Che, and J. L. Krause, Chem. Phys. **217**, 297 (1997).
[35] Y. J. Yan, J. S. Cao, and Z. W. Shen, J. Chem. Phys. **107**, 3471 (1997).
[36] J. X. Cheng, Z. W. Shen, and Y. J. Yan, J. Chem. Phys. **109**, 1654 (1998).
[37] I. Averbukh and M. Shapiro, Phys. Rev. A **47**, 5086 (1993).
[38] L. Y. Shen, S. H. Shi, and H. Rabitz, J. Phys. Chem. **97**, 12,114 (1993).
[39] V. Dubov and H. Rabitz, Phys. Rev. A **54**, 710 (1996).
[40] Y. J. Yan, L. E. Fried, and S. Mukamel, J. Phys. Chem. **93**, 8149 (1989).
[41] Y. J. Yan and S. Mukamel, Phys. Rev. A **41**, 6485 (1990).
[42] S. Mukamel, *The Principles of Nonlinear Optical Spectroscopy* (Oxford University Press, New York, 1995).
[43] L. Allen and J. H. Eberly, *Optical Resonance and Two-level Atoms* (Dover, New York, 1987).
[44] J. S. Cao, C. J. Bardeen, and K. R. Wilson, Phys. Rev. Lett. **80**, 1406 (1998).
[45] S. Chelkowski, A. Bandrauk, and P. B. Corkum, Phys. Rev. Lett. **65**, 2355 (1990).
[46] D. Goswami and W. S. Warren, J. Chem. Phys. **99**, 4509 (1993).
[47] C. Liedenbaum, S. Stolte, and J. Reuss, Phys. Rep. **178**, 1 (1989).
[48] J. S. Melinger, A. Hariharan, S. R. Gandhi, and W. S. Warren, J. Chem. Phys. **95**, 2210 (1991).
[49] E. T. J. Nibbering, D. A. Wiersma, and K. Duppen, Phys. Rev. Lett. **68**, 514 (1992).
[50] K. Duppen, F. de Haan, E. T. J. Nibbering, and D. A. Wiersma, Phys. Rev. A **47**, 5120 (1993).
[51] G. Cerullo, C. J. Bardeen, Q. Wang, and C. V. Shank, Chem. Phys. Lett. **262**, 362 (1996).